ELSEVIER

Journal of Structural Geology 27 (2005) 679–692

JOURNAL OF STRUCTURAL GEOLOGY

www.elsevier.com/locate/jsg

Rotation behaviour of rigid inclusions in multiple association: insights from experimental and theoretical models

Nibir Mandal[a], Susanta Kumar Samanta[a], Gautam Bhattacharyya[a], Chandan Chakraborty[b,*]

[a]*Department of Geological Sciences, Jadavpur University, Kolkata 700032, India*
[b]*Geological Studies Unit, Indian Statistical Institute, 203, B.T. Road, Kolkata 700108, India*

Received 28 June 2004; received in revised form 10 November 2004; accepted 13 November 2004
Available online 17 March 2005

Abstract

Many rocks are representative of inclusion–matrix systems where rigid inclusions float on a ductile matrix. The geological analogues of such inclusion–matrix systems are theoretically modelled with the help of Jeffery's (1922) theory. In recent years, there have been a number of reinvestigations on the rotational motion of rigid inclusions to account for some geological observations that are not yet predicted in models based on Jeffery's theory. Adding to this effort, this paper investigates the effects of (1) inclusion concentration and (2) the degree of coherence at the inclusion–matrix interface on the rotation behaviour of rigid inclusions in a multiple inclusion system during simple shear deformation. Shear-box experiments were run on models containing multiple, identical elliptic cylinders of wax mimicking rigid inclusion embedded within putty representing ductile matrix. Two sets of experiments were performed, with and without lubrication at the inclusion–matrix interfaces. Each model had an isolated inclusion to reveal the variation of rotations of single and multiple inclusions. Increase in inclusion concentration (α) results in contrasting rotation behaviour of isolated and multiple inclusions initially oriented parallel to the shear direction. When the interfaces were not lubricated, inclusions in multiple association rotated antithetically, whereas the isolated one almost remained stationary. In models wherein the inclusion–matrix interfaces were lubricated with liquid soap, both isolated and multiple inclusions rotated antithetically, but the isolated inclusion rotated at a lower rate. With increasing inclusion concentration, the difference in the rates of antithetic rotation between isolated and multiple inclusions tended to be larger in both lubricated and non-lubricated conditions. The sense of rotation of isolated as well as multiple inclusions, initially oriented perpendicular to the shear direction, was always synthetic irrespective of the nature of the interface (lubricated or non-lubricated); however, the instantaneous rotation rates of inclusions in multiple association were higher than that of the isolated inclusions disposed in the same orientation.

Rotation of inclusion in an inclusion–matrix system is basically induced by the traction exerted by the flowing matrix on the surface of the inclusion during deformation. Employing a hydrodynamic model it is shown that mutual mechanical interaction among inclusions, which is a function of inclusion concentration (α), modifies the stresses at the inclusion–matrix interface to a large extent. Moment calculations reveal that inclusions oriented parallel to the shear direction experience an antithetic moment in response to the normal stress components, the magnitude of which increases with increasing inclusion concentration. This implies that rotation of shear-parallel inclusions in antithetic sense is favoured by higher inclusion concentration. On the other hand, inclusions oriented perpendicular to shear direction experience a moment that induces synthetic rotation. The magnitude of the synthetic moment is larger for larger inclusion concentration leading to increase in the rate of synthetic rotation. Using the theoretical model, the moments are calculated as a function of the aspect ratio of inclusions and the inferences based on this moment calculation are complemented with experimental findings.

Keywords: Rigid inclusion; Inclusion concentration; Shear; Antithetic rotation; Synthetic rotation; Moment

1. Introduction

Understanding the rotational motion of rigid bodies within a flowing viscous matrix and their governing physical parameters is essential to analyse many structures in deformed rocks, such as porphyroclast mantle, porphyroblast trail, development of stable fabric etc. A plethora of

* Corresponding author
E-mail address: chandan@isical.ac.in (C. Chakraborty).

0191-8141/$ - see front matter © 2005 Elsevier Ltd. All rights reserved.
doi:10.1016/j.jsg.2004.11.007

theoretical models have evolved in this subject over the last couple of decades that quantitatively describe the motion of rigid objects in progressive deformation, depending on two parameters: (1) the shape and orientation of rigid objects and (2) the velocity gradient tensor of bulk flow (Gay, 1968a,b; Ghosh and Ramberg, 1976; Freeman, 1985; Passchier, 1987, 1994; Masuda et al., 1995; Jezek et al., 1996; Pennacchioni et al., 2000; Mandal et al., 2001a). A basic premise in these analyses is that the object remains attached to the matrix. According to these models, during progressive simple shear a coherent object would continuously rotate in synthetic sense. However, the rotational motion of rigid inclusions could significantly vary depending on the mechanical setting of inclusion–matrix systems (e.g. Bjornerud and Zhang, 1995). For example, Stewart (1997) suggested from analogue models that, under special circumstances, rigid inclusions might remain stationary during progressive deformation (cf. Bell, 1985; Bell and Johnson, 1989; Bell and Hickey, 1997). On the other hand, a number of workers have shown that, in inclusion–matrix systems with low coherence, the inclusions may rotate antithetically, and they may acquire a fixed orientation defining a stable fabric (Ildefonse and Mancktelow, 1993; Marques and Coelho, 2001; Mancktelow et al., 2002; Ceriani et al., 2003; Marques and Bose, 2004; Schmid and Podladchikov, 2004), which cannot be accounted for in the theoretical models mentioned above. Antithetic rotation of rigid inclusion with incoherent interface has been clearly documented in experiments with a single inclusion (Marques and Coelho, 2001; Mancktelow et al., 2002; Ceriani et al., 2003). The experimental results of Ildefonse and Mancktelow (1993) indicate that rigid inclusions may rotate antithetically in multiple inclusion systems too. In such a situation, in addition to inclusion–matrix coherence, mutual interaction among inclusions would be another controlling factor governing the rotational motion of rigid inclusions (cf. Samanta et al., 2003). The mechanics of antithetic rotation of rigid inclusions in a multiple inclusion system is yet to be fully explored and demands a suitable dynamic analysis for a reasonable physical explanation of the phenomenon.

Following the work of Ildefonse et al. (1992a,b), who dealt with multiple inclusions, we examine, with the help of analogue models, the rotational motion of rigid inclusions in a multiple inclusion system as a function of inclusion concentration and inclusion–matrix coherence. The paper also presents a hydrodynamic theory to show the influence of mechanical interaction on the moment of individual inclusions that effectively governs the rotational motion of the inclusions in a bulk simple shear deformation in response to the traction on them asserted by the flowing matrix. The theoretical analysis allows us to determine the rotational motion of inclusions as a function of their concentration and aspect ratio. Though not attempted here, the findings of this paper may be utilized to understand development of stable fabric in multiple inclusion systems (Mancktelow et al., 2002; Ceriani et al., 2003; Schmid and Podladchikov, 2004).

2. Analogue models

2.1. Experimental method

We designed our experimental models following the method of earlier workers (Ildefonse and Mancktelow, 1993). A number of identical elliptic cylindrical rigid inclusions, made up of wax, were embedded in a ductile matrix of putty (viscosity $\sim 10^5$ Pa s; Fig. 1). Two sets of experiments were performed with lubricated and non-lubricated inclusion–matrix interfaces. The interfaces were lubricated with liquid soap. During simple shear deformation detachment developed at the inclusion–matrix interfaces, forming fissures on either side of the inclusion whether or not the interface was lubricated (Fig. 2). We used markers across the inclusion–matrix interface and tested the degree of incoherence considering the surface area of detachment. It was found that for a finite deformation the proportion of detached area significantly increased in case of lubricated interface, implying a reduction of inclusion–matrix coherence (Fig. 2). Moreover, inclusions with lubricated interface and oriented parallel to the shear direction rotated antithetically, supporting the existing notion that low coherence between inclusion and matrix

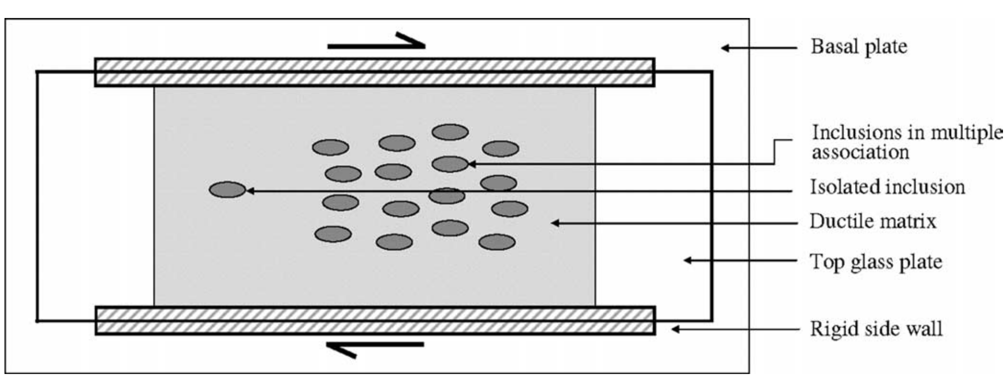

Fig. 1. Schematic sketch (plan view) of experimental set-up for model deformation in simple shear.

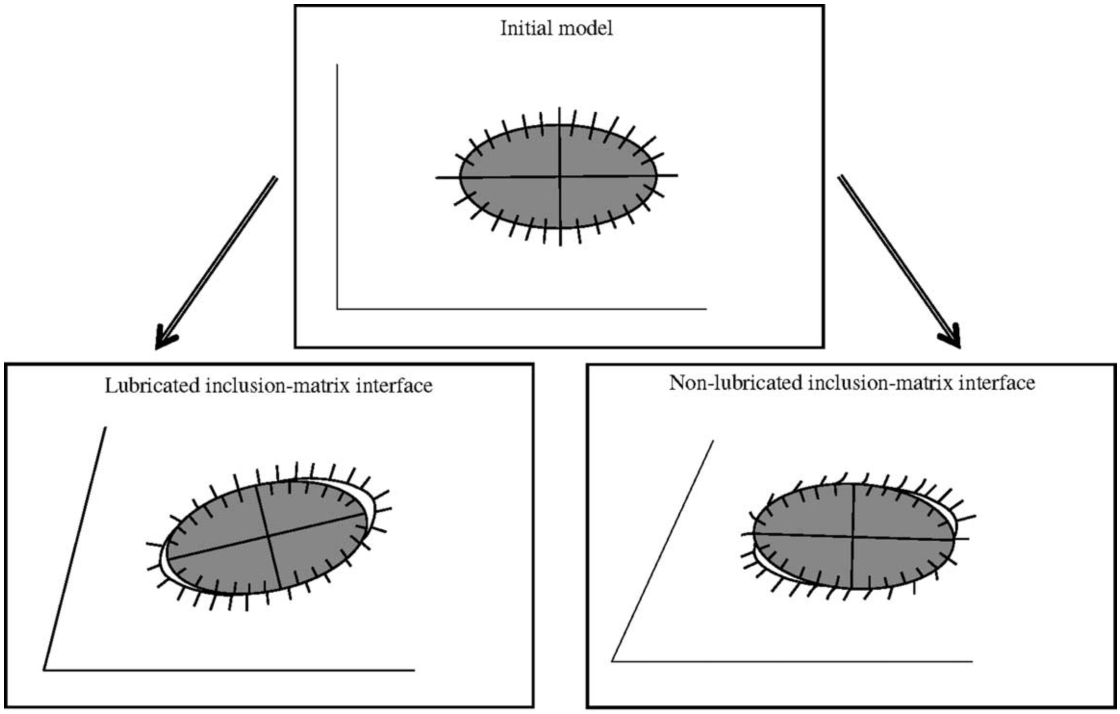

Fig. 2. Sketches from deformed physical models containing single inclusion to show the difference in the area and mode of detachment due to lubricated and non-lubricated conditions at the interface. Note that in the case of a lubricated interface the proportion of detachment (extensional and slip) is much more than around the inclusion without lubrication. Also notice that enhancement of detachment promoted antithetic rotation of the inclusion.

promotes antithetic rotation (Marques and Coelho, 2001; Mancktelow et al., 2002; Ceriani et al., 2003).

For a particular condition of inclusion–matrix interface (lubricated or non-lubricated), we ran experiments in a shear box by varying inclusion concentration in two sets: one with the long axes of inclusions oriented parallel and the other perpendicular to the shear direction. In each experimental run an inclusion was kept away from the association of multiple inclusions to observe the difference in rotation behaviour between a single inclusion and those in interacting state.

2.2. Experimental results

2.2.1. Inclusions with lubricated interface

In experiments with inclusions oriented parallel to the shear direction, the sense of rotation of single as well as multiple inclusions was always antithetic as observed in earlier studies (Ildefonse and Mancktelow, 1993; Marques and Coelho, 2001; Mancktelow et al., 2002; Ceriani et al., 2003). This study, in addition, reveals that the magnitude of antithetic rotation for a given finite shear is sensitive to inclusion concentration, as reflected in the lower rotation of the single inclusion kept in isolation from the multiple inclusions (Fig. 3). Moreover, at every instant of progressive shearing the isolated inclusion was reoriented antithetically at an angle (with respect to the shear direction) less than that of inclusions in multiple associations. It was noticed that the antithetic rotation of inclusions in multiple associations tends to cease in the course of progressive shearing, which may eventually lead to development of a stable fabric making an angle ($\sim 24°$) to the shear direction (cf. Mancktelow et al., 2002; Ceriani et al., 2003; Schmid and Podladchikov, 2004). With decrease in inclusion concentration the rate of antithetic rotation reduced and the difference in rotation between inclusions occurring in multiple and single states tended to be small (Fig. 4a).

We performed similar experiments with inclusions oriented at a right angle to the bulk shear direction (Fig. 5a). In these experiments inclusions in multiple as well as single states rotated synthetically, but at different rates (Fig. 5b). Experiments with large inclusion concentrations show that those in multiple associations rotate faster than the isolated inclusion, suggesting that the mechanical interaction among inclusions promote their synthetic rotation. The difference in the rotation rate tends to decrease as the inclusion concentration is reduced (Fig. 4b).

2.2.2. Inclusions with non-lubricated interface

The inclusions were initially attached to the matrix. However, during deformation detachment formed locally at the inclusion–matrix interface, involving both slip movement and extensional fissures on either side of them, making the interface partially incoherent (cf. Samanta and Bhattacharyya, 2003). Our experiments were designed to test how such partial coherence subsequently influences the rotation behaviour of inclusions in multiple associations. The inclusions oriented parallel to the shear direction and

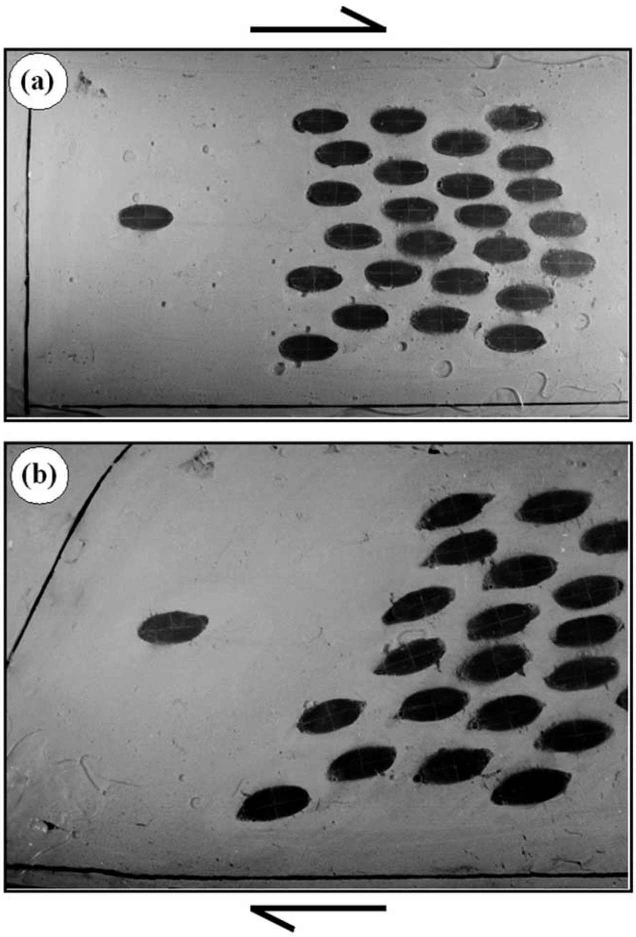

Fig. 3. Rotation of rigid inclusions ($R=2$) with lubricated interfaces in physical experiments under dextral shear. (a) Initial model containing inclusions oriented parallel to the shear direction in high concentration (∼40% in area). (b) Deformed model showing antithetic rotation of isolated as well as multiple inclusions. Finite shear: 0.5. Note that inclusions occurring in the central portion of the cluster have rotated larger than the isolated and the peripheral inclusions. Long dimension of inclusions: 2 cm.

occurring in multiple association rotated significantly in antithetic sense following development of detachment (Fig. 6). On the other hand, the isolated inclusion did not show any significant antithetic rotation even when there was slip as well as extensional detachment at its interfaces, developing fissures on either side. The rate of antithetic rotation of multiple inclusions in this case was, however, less than that observed in the previous models with lubricated interface. Decreasing inclusion concentration in the model results in reduction of the rotation rate of multiple inclusions (Fig. 7).

In the following section we present a theory to show how the mechanical interaction, which is a function of inclusion concentration, promotes antithetic rotation of inclusions oriented parallel to the direction of bulk shear. The theory imposes the condition of low mechanical strength at the inclusion–matrix interface simulating the experimental models with lubricated interfaces.

3. Theory

3.1. Mathematical considerations

Consider a two-dimensional system containing multiple elliptical rigid inclusions, which are randomly distributed but uniformly oriented with long axes parallel to the direction of bulk shear (Fig. 8a). All the inclusions are assumed to be identical in shape with semi-axes a and b. In order to analyse the effect of inclusion concentration on the rotation behaviour of inclusions in an interacting state we employ the method of moment calculation on individual inclusions. This involves derivation of the flow field around an inclusion in an interacting state (cf. Samanta et al., 2003). In determining the flow field, a Cartesian coordinate frame xy is chosen at the centre of an inclusion with x-axis along the a-axis of inclusion. A concentric ellipse is considered around the inclusion defining its mean boundary of mutual interaction with the neighbouring inclusions. The boundary conditions of mechanical interaction are imposed on this elliptical boundary (Happel, 1957). In this analysis we will refer to xy space as z-space (Fig. 8b). In the z-space the boundary of inclusion is expressed as:

$$\frac{x^2}{a^2}+\frac{y^2}{b^2}=1 \tag{1}$$

For the sake of mathematical treatment the z-space is converted to another space, described as ψ space employing the conformal transformation method, where an elliptical contour in the z-space describes a circle in the ψ space (Fig. 8b). The mathematical equation of this transformation follows:

$$z=\omega(\psi)=\lambda_1\left(\psi+\frac{\lambda_2}{\psi}\right),\quad z=x+iy \tag{2}$$

where λ_1 and λ_2 are two transformation factors and

$$\psi=\rho e^{i\phi} \tag{3}$$

ρ and ϕ are polar coordinates in ψ space. The elliptical inclusion with semi-axes, a and b, is projected in the ψ space as a circle with a radius ρ_1. Using Eqs. (2) and (3), we find:

$$a=\lambda_1\left(\rho_1+\frac{\lambda_2}{\rho_1}\right)\quad\text{and}\quad b=\lambda_1\left(\rho_1-\frac{\lambda_2}{\rho_1}\right) \tag{4}$$

The concentric boundary ellipse is accordingly transformed to a circle with a radius ρ_2. Therefore, the ratio ρ_1/ρ_2 proxies the measure of inclusion concentration in the system. The factors λ_1 and λ_2 in the conformal transformation are:

$$\lambda_1=\frac{R+1}{2}\frac{b}{\rho_1}\quad\text{and}\quad\lambda_2=\frac{R-1}{R+1}\rho_1^2$$

R is the axial ratio of the ellipse. We impose the conditions of mechanical interaction of neighbouring inclusions at the contours $\rho=\rho_2$ in ψ space, as given in Eq. 3 of Happel

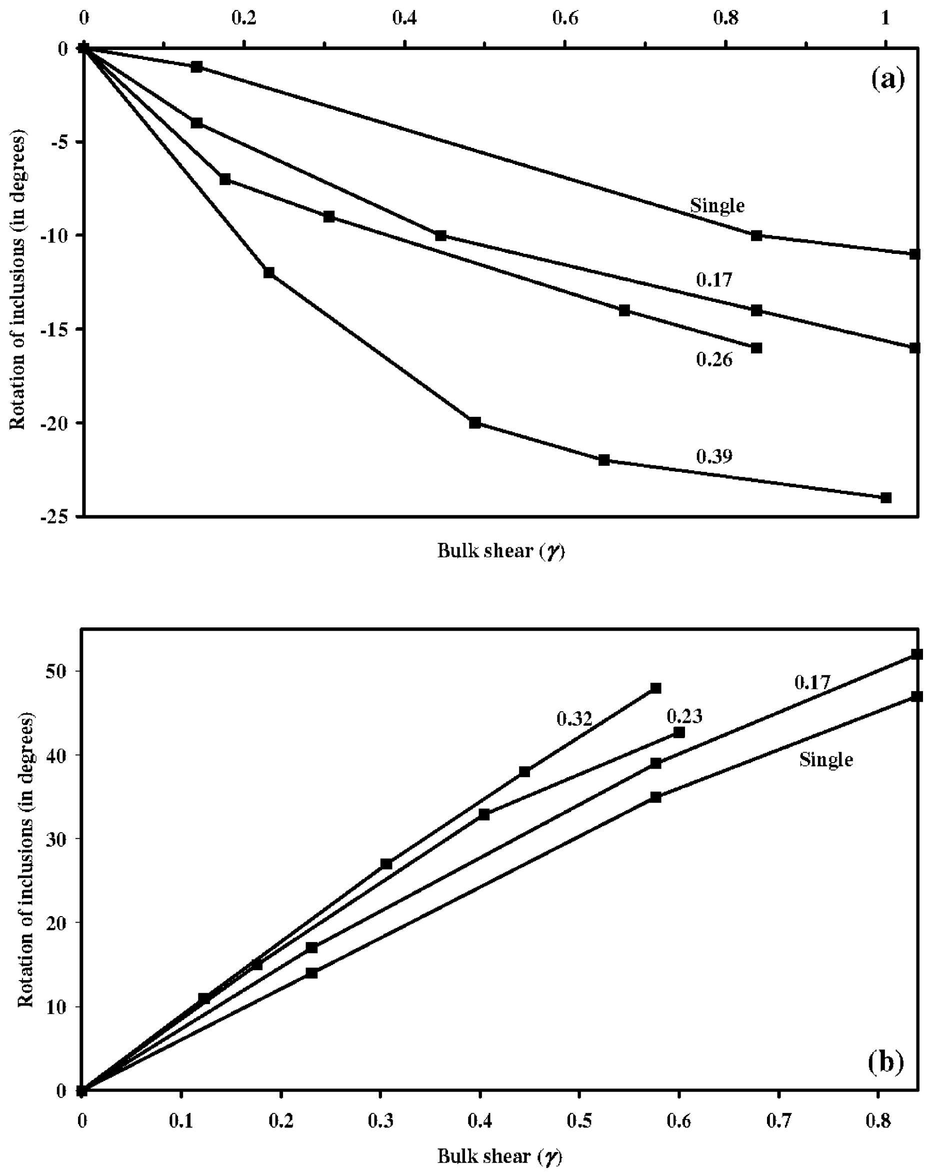

Fig. 4. Plots of finite rotation of multiple inclusions with finite bulk shear in experimental models. The inclusions were initially oriented (a) parallel and (b) perpendicular to the shear direction. The average value of their rotation was considered for the plot. Numerical values corresponding to the curves represent the inclusion concentration in area proportion. $R=2$. Notice that for any finite bulk shear, the rotation of inclusions is larger for higher concentrations.

(1957), which considers no perturbed normal flow across the contour, and vanishing shear stress component. Employing these conditions, we can obtain the stress at any point in the neighbourhood of inclusion in the ψ space as:

$$\sigma_{\rho\rho} = \left(-6\rho^2 A + 4B - 36\frac{C}{\rho^3} + 24\frac{D}{\rho^5} + 2\right)\eta\dot{\gamma}\sin\phi\cos\phi$$
$$\sigma_{\phi\phi} = (-70\rho^2 A - 4B - 14\frac{D}{\rho^5} - 2)\eta\dot{\gamma}\sin\phi\cos\phi \tag{5}$$

A, B, C and D are constants, and their expressions depend on the concentration parameter α, where $\alpha=\rho_1/\rho_2$ (Mandal et al., 2004).

We can transform the stress functions in the z-space considering the following equations (Mushkhelishvilli, 1953):

$$\sigma_{xx} + \sigma_{yy} = \sigma_{\rho\rho} + \sigma_{\phi\phi} \tag{6a}$$

$$\sigma_{yy} - \sigma_{xx} + 2i\sigma_{xy} = \left(\sigma_{\phi\phi} - \sigma_{\rho\rho} + 2i\sigma_{\rho\phi}\right)e^{-2i\alpha} \tag{6b}$$

where

$$e^{2i\alpha} = \frac{\psi^2}{\rho^2}\frac{\omega'(\psi)}{\overline{\omega'(\psi)}}, \quad \omega(\psi) = \frac{d}{d\psi}\{\omega(\psi)\} \tag{7}$$

The bar over the function in the numerator of Eq. (7) represents conjugate of the function. From Eqs. (2) and (7) we have:

$$e^{2i\alpha} = \frac{e^{2i\phi} - \frac{\lambda_2}{\rho^2}}{1 - \frac{\lambda_2}{\rho^2}e^{-2i\phi}} \tag{8}$$

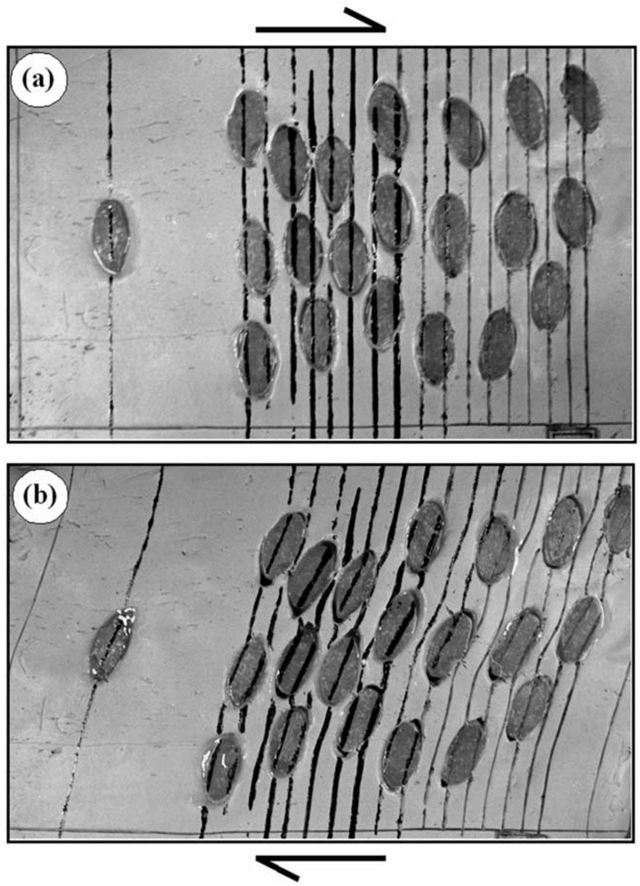

Fig. 5. Synthetic rotation of multiple inclusions with lubricated interfaces in experimental models under dextral shear. The inclusions were initially oriented perpendicular to the shear direction. Note that central inclusions in the multiple associations (right) have rotated larger than the isolated inclusion (left). Inclusion concentration $\sim$35% in area. R=2. Finite shear 0.3. Long dimension of inclusions: 2 cm.

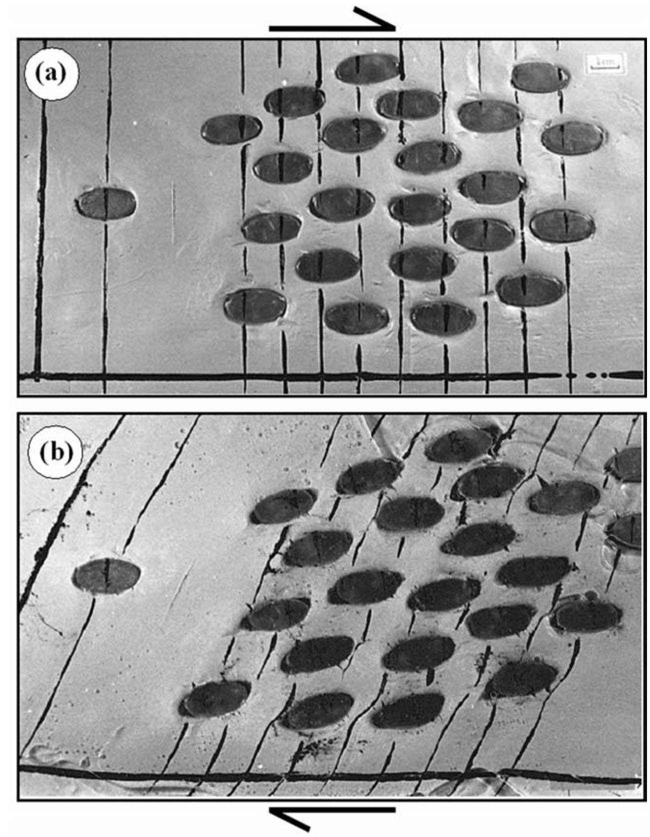

Fig. 6. Antithetic rotation of multiple inclusions in physical models with non-lubricated interfaces. (a) Initial model. (b) Deformed model (finite shear 0.36). Notice that the isolated inclusion (left) has remained virtually stationary, whereas the inclusions in multiple associations rotated antithetically. Inclusion concentration 30% in area. Long dimension of inclusions: 2 cm. Notice that for any finite bulk shear the rotation of inclusions is larger for higher concentrations.

Eq. (8) follows:

$$\sigma_{xx} = \frac{\sigma_{\rho\rho} + \sigma_{\phi\phi}}{2} + \frac{\sigma_{\rho\rho} - \sigma_{\phi\phi}}{2}\cos 2\alpha - \sigma_{\rho\phi}\sin 2\alpha,$$
$$\sigma_{yy} = \frac{\sigma_{\rho\rho} + \sigma_{\phi\phi}}{2} - \frac{\sigma_{\rho\rho} - \sigma_{\phi\phi}}{2}\cos 2\alpha - \sigma_{\rho\phi}\sin 2\alpha, \quad (9)$$
$$\sigma_{xy} = \frac{\sigma_{\rho\rho} - \sigma_{\phi\phi}}{2}\sin 2\alpha + \sigma_{\rho\phi}\cos 2\alpha$$

In order to determine the moment in inclusion we need to consider the traction vector $\mathbf{T}_\mathrm{i}$ at the surface of inclusion in the z-space. It follows from Cauchy's equation:

$$\mathbf{T}_\mathrm{i} = \sigma_{ij}\mathbf{n}_j \quad (10)$$

where $i,j = x,y$ and $\mathbf{n}$ is the unit normal vector to the plane of interest.

$$\mathbf{n}_\mathrm{i} = \begin{bmatrix}\cos\theta \\ \sin\theta\end{bmatrix} \quad (11)$$

θ is the inclination of $\mathbf{n}_\mathrm{i}$ to the x-axis. With the help of Eqs. (8)–(11), we can find the normal and shear stress components on this plane as:

$$\sigma = \frac{\sigma_{\rho\rho} + \sigma_{\phi\phi}}{2} + \frac{\sigma_{\rho\rho} - \sigma_{\phi\phi}}{2}\cos 2(\alpha - \theta) - \sigma_{\rho\phi}\sin 2(\alpha - \theta), \quad (12)$$
$$\tau = \frac{\sigma_{\rho\rho} - \sigma_{\phi\phi}}{2}\sin 2(\alpha - \theta) + \sigma_{\rho\phi}\cos 2(\alpha - \theta)$$

We now determine moments in the inclusion resulting from the normal stress σ and the shear stress τ that act on the surface of inclusion. Consider a small surface element ds with unit normal vector $\mathbf{n}_\mathrm{i}$ on the surface of inclusion (Fig. 9a). d is the perpendicular distance of the normal vector from the centre of inclusion. Moment due to the normal stress σ is: $dM_\mathrm{n} = d\sigma ds$, which can be presented in terms of the Cartesian coordinates as:

$$dM_\mathrm{n} = \sqrt{x^2 + y^2}\sin(\theta - \beta)\sigma ds \quad (13)$$

Similarly, moment due to the shear stress τ (Fig. 9b) can be derived as:

$$dM_\mathrm{t} = \sqrt{x^2 + y^2}\cos(\theta - \beta)\tau ds \quad (14)$$

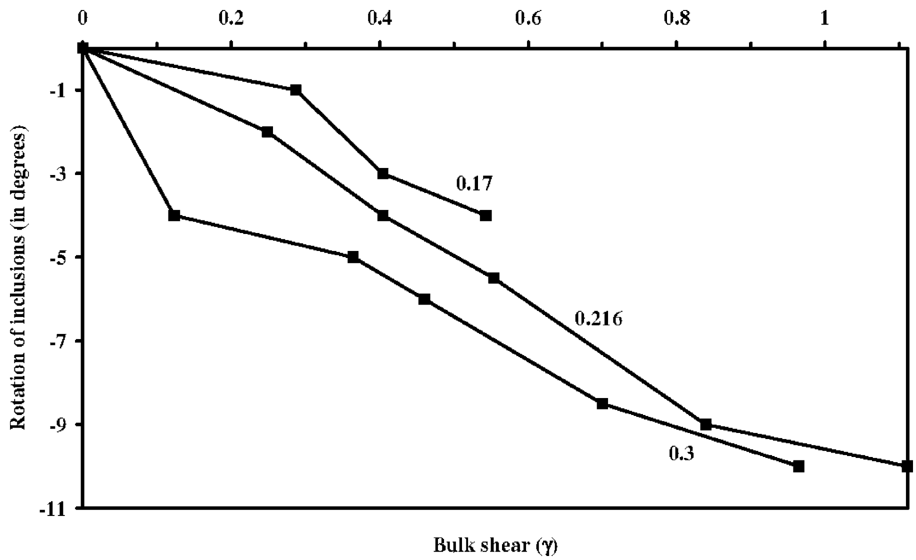

Fig. 7. Plot showing rotation of multiple inclusions with non-lubricated interface during progressive shear in physical experiments for different inclusion concentrations.

Differentiating Eq. (1) and after some algebraic manipulations, $(\theta-\beta)$ is obtained in terms of Cartesian coordinates as:

$$\tan(\theta-\beta)=\frac{R^2-1}{a^2}xy \quad (15)$$

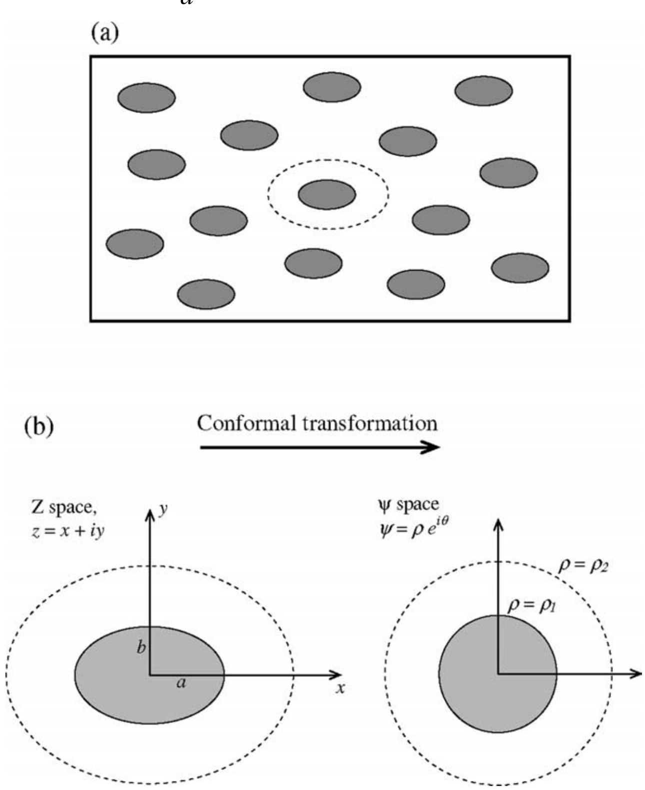

Fig. 8. (a) Consideration of inclusion–matrix system for theoretical analysis. Dashed line marks the boundary on which the conditions for mutual interaction with the neighbouring inclusions are imposed. (b) Conformal transformation of the real space (z-space) to ψ-space. Details are cited in text.

where R is the aspect ratio of inclusion. Eqs. (13) and (14) can be integrated to find the total moment resulting from the normal and the stress components on the inclusion. We calculated these moments numerically using a computer programme on Visual Basic. The numerical analysis involved coordinate transformation from z to ψ space using Eq. (2), and the stress components were determined in ψ space from Eq. (5). We then transformed all the stress components to z-space, and calculated the moments. It is evident from Eq. (5) that the normal and shear stresses acting at the inclusion–matrix interface are functions of inclusion concentration in the system. In our numerical calculations, for convenience α is chosen as a measure of concentration, where $\alpha=\rho_1/\rho_2$. The value of α tends to be zero, simulating a single inclusion system. On the contrary, when it approaches one, it implies a system with densely packed inclusions remaining in contact with one another (Mandal et al., 2003). The magnitudes of both normal and shear stresses increase with increasing inclusion concentration. However, the increase of normal stress component is larger than that of the shear stress component (Fig. 10). In the following section we show how inclusion concentration thereby promotes antithetic rotation of inclusions oriented parallel to the bulk shear direction.

3.2. Analysis of inclusion rotation

We ran a set of computational runs to find the moment on inclusions that determines the instantaneous rotation of inclusion, setting extremely low coherence to the matrix, i.e. the interfaces were considered to have zero tensile (T_0) and shear strength (S_0), and also to be frictionless. In such a situation the shear stress will exert no moment but the compressive normal stress component will be the moment inducing factor that would rotate the inclusion (Eq. (13)). For

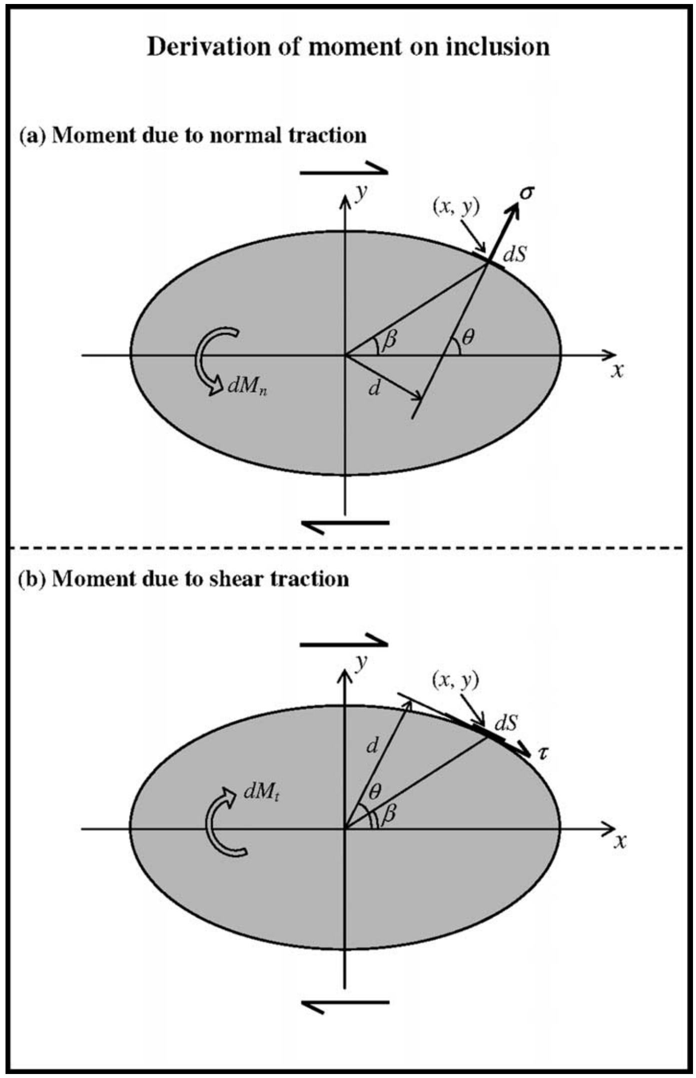

Fig. 9. Derivations of the moments on inclusion developed in response to (a) normal and (b) shear traction exerted by the flowing matrix. See text for details.

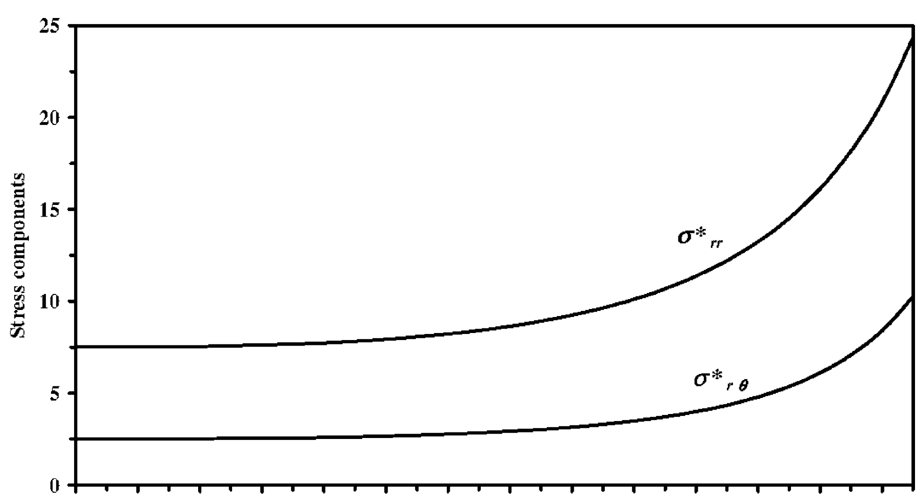

Fig. 10. Variations of the maximum normal stress (σ^*_{rr}) and shear stress ($\sigma^*_{r\theta}$), normalized to bulk flow stress, with inclusion concentration.

a non-zero value of α, the moment is found to be negative, and thereby drives the inclusion to rotate antithetically. For a given aspect ratio, the magnitude of negative moment increases with increasing inclusion concentration (Fig. 11a), indicating that inclusions occurring in high concentrations are likely to show larger antithetic rotation, as observed in physical experiments. Moment versus concentration plots suggest that the effect of inclusion concentration becomes more pronounced when the value of concentration parameter is higher than 0.4, above which the moment increases with increasing gradients. The analytical results conform to our experimental finding, where the difference in antithetic rotation between isolated inclusions and those occurring in clusters is larger for large inclusion concentration (Fig. 4).

The variation of antithetic moment with inclusion concentration depends also on the aspect ratio (R) of inclusion (Fig. 11b). For a given concentration, the magnitude of moment increases with R, but tends to assume an asymptotic value. The variation implies that the instantaneous antithetic rotation will be insensitive to aspect ratio when the latter becomes large. In order to verify this theoretical result we conducted a few physical experiments on multiple inclusion systems considering two clusters of inclusions with aspect ratios 2 and 4, respectively. The

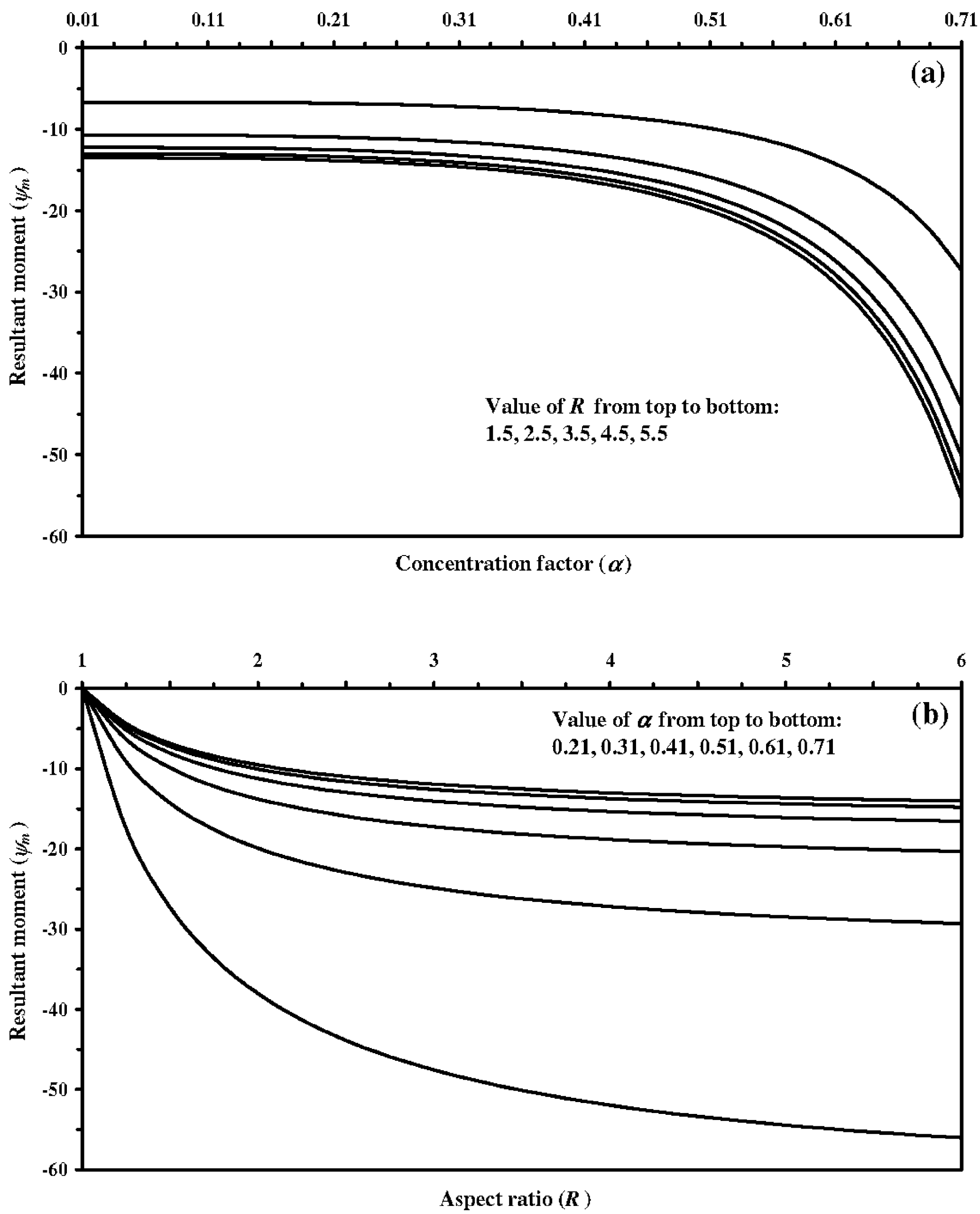

Fig. 11. (a) Calculated plots of the resultant moment (ψ_m) in incoherent inclusion as a function of inclusion concentration α; (b) Moment versus aspect ratio plots for different inclusion concentrations. $S_0^* = T_0^* = 0$. $R = a/b$. The moment considered here is dimensionless, as it is calculated with the traction components normalized to the bulk flow stress and divided by ab, where a and b are the axial dimensions of inclusion.

experiments show that shear-parallel inclusions with aspect ratio 4 had an instantaneous antithetic rotation more than that of inclusions with aspect ratio 2 (Fig. 12). The difference in rotation is, however, small, which can also be predicted from the theoretical curve. With progressive shearing this was further reduced, as the inclusions of lower aspect ratio continued to rotate, whereas those of higher aspect ratio ceased to rotate.

Numerical simulations were also run imparting strengths

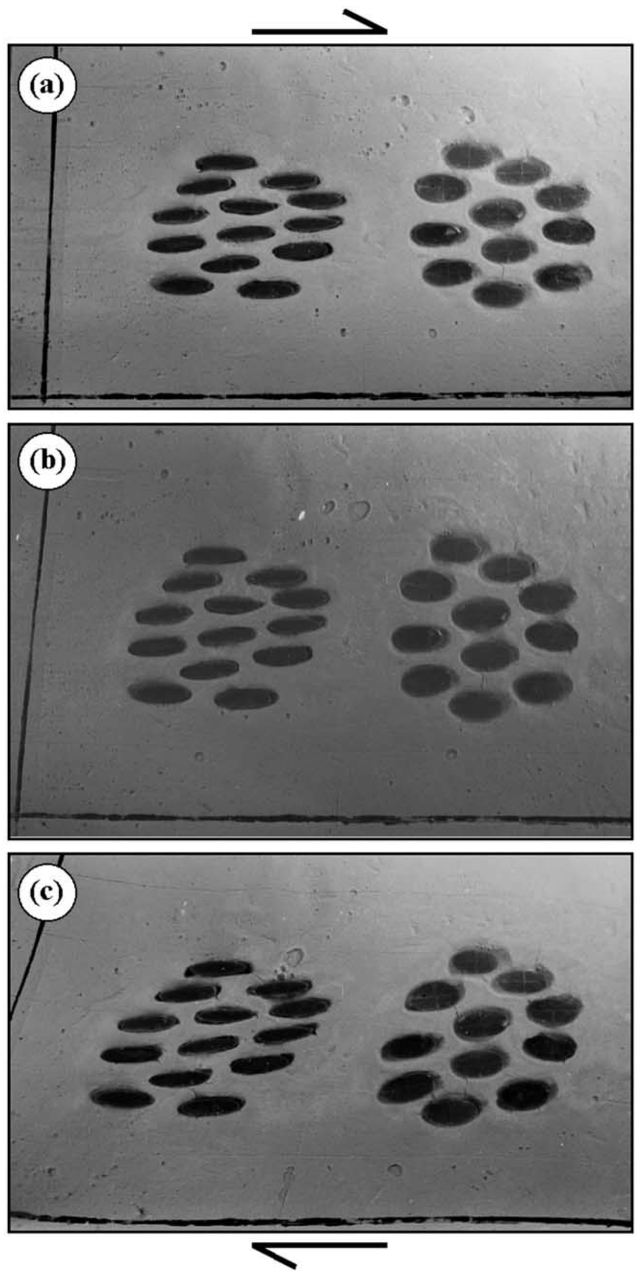

Fig. 12. Three successive stages of shear deformation of a model containing two clusters of multiple inclusions, one of aspect ratio $R=2$ (right) and the other $R=4$ (left). Note that inclusions (central) of larger aspect ratio have rotated slightly faster at the initial stage. Long dimension of inclusions of aspect ratio 2 is 2 cm.

at the interfaces. It was revealed that for a given inclusion concentration the magnitude of antithetic moment decreases with increasing strengths of inclusion–matrix interfaces (Fig. 13). Thus, for any volume concentration the instantaneous antithetic rotation will be lower for higher inclusion–matrix coherence, which conform to our findings from physical models (Fig. 6b). However, the variation in moment due to different coherence is reduced when the inclusion concentration is large.

The same theory can be used to analyse the rotation behaviour of inclusions oriented perpendicular to the shear direction by considering the conformal transformation (Eq. (2)) as:

$$z = \omega(\psi) = \lambda_1\left(\psi - \frac{\lambda_2}{\psi}\right) \tag{16}$$

We did similar analysis considering the conformal transformation in Eq. (16). Numerical calculations reveal that the moment of a perpendicularly oriented incoherent inclusion in multiple inclusion systems is positive, and its magnitude increases non-linearly with increasing inclusion concentration (Fig. 14a). This supports our experimental findings that inclusions forming a cluster rotate synthetically faster than single, isolated inclusions in the same model (Fig. 5b). The effect of inclusion concentration in promoting synthetic rotation is a function of aspect ratio. For a given concentration, the moment increases with aspect ratio, attains a maximum value and then decreases with further increase in aspect ratio (Fig. 14b). This implies that the effect of concentration in synthetic rotation will be less for large aspect ratios. We conducted experiments on models containing two clusters of inclusions with aspect ratio 2 and 4. These experiments clearly show that the synthetic rotation of inclusions with aspect ratio 2 is discernibly faster than that of inclusions with aspect ratio 4 (Fig. 15). The finding supports the results obtained from the theory. It appears that the topology of the inclusion–matrix system with inclusions of lower aspect ratios (~ 2) favours intensification of the compressive stresses arising from the mutual interaction of inclusion. This increase in compressive stress normal to the surface of inclusion promotes the rate of synthetic rotation of inclusions of aspect ratio 2 occurring in multiple associations.

4. Discussion

Recent experimental studies on single inclusion systems mentioned in Section 1 reveal that mechanical condition at the inclusion–matrix interface (coherent or incoherent) is a crucial factor in determining the rotational motion of rigid inclusions (Marques and Coelho, 2001; Mancktelow et al., 2002; Ceriani et al., 2003). In the case of extremely low inclusion–matrix coherence the inclusions can rotate antithetically in simple shear, which is not predicted from

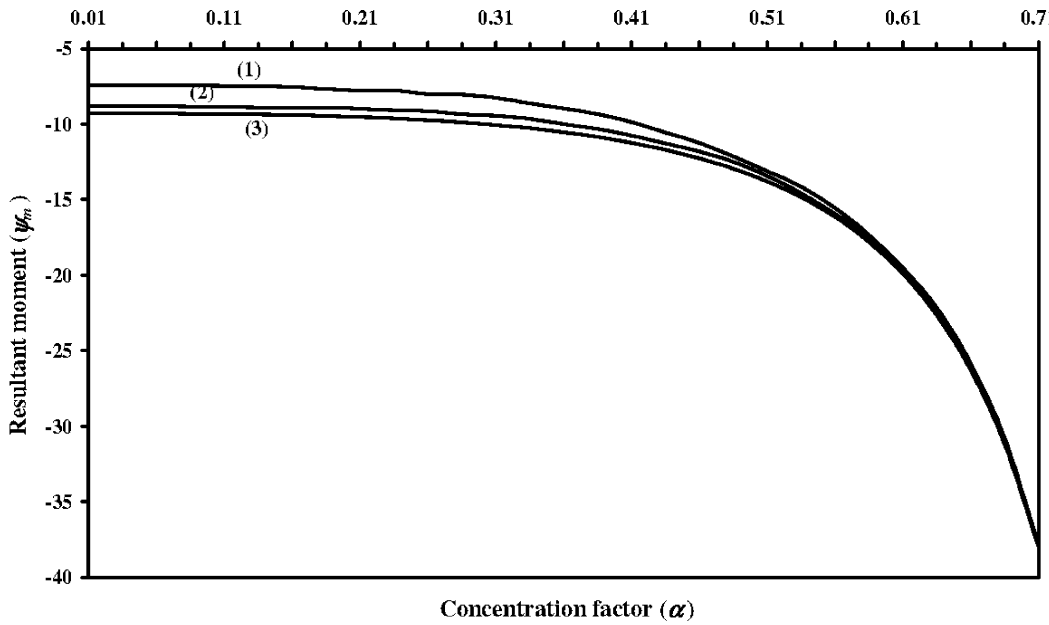

Fig. 13. ψ_m versus α plots for three different inclusion-matrix coherence. (1) $S_0^* = 2$, $T_0^* = 1$; (2) $S_0^* = 1.5$, $T_0^* = 1$ and (3) $S_0^* = T_0^* = 0$.

Jeffery's (1922) theory for coherent inclusions. The prime aim of this paper is to advance the findings for multiple inclusion systems and explore how the mechanical interaction, a function of inclusion concentration, can additionally influence the rotational motion of rigid inclusions with low coherence to the matrix. In experiments, inclusions with the long axis oriented parallel and perpendicular to the shear direction rotate antithetically and synthetically, respectively, as documented in earlier studies on single inclusion systems. The magnitudes of antithetic and synthetic rotation are found to be larger in the case of multiple inclusions and the difference increases with increasing inclusion concentration. Our study suggests that the effect of inclusion–matrix incoherence in the development of clast-associated structures, e.g. fissures around rigid porphyroblasts, foliation drag, will be more effective in rocks containing clasts in large volume concentrations.

We used liquid soap as lubricating material at the inclusion–matrix interfaces in the experimental models. This was merely to reduce the cohesion strength of inclusion–matrix interfaces, as in earlier experiments (Mancktelow et al., 2002). Comparing the results obtained from experiments on models with and without lubrication, it is evident that the effect of inclusion concentration in promoting antithetic rotation would be more pronounced for further low inclusion–matrix coherence. Our study demonstrates that reverse rotation of inclusions is possible in multiple inclusion systems even when the interface strength is not extremely low, a necessary condition for such motion in single inclusion systems.

Both the experimental and theoretical models are based on inclusions elliptical in shape. However, natural clasts often show non-elliptical geometry (Treagus and Lan, 2003). Physical experiments clearly demonstrate that a non-elliptical, asymmetrical shape of inclusions exerts additional effects on the rotational behaviour of rigid inclusions with weak interfaces (Mancktelow et al., 2002; Ceriani et al., 2003). Based on these experimental observations it appears that a non-elliptical shape would be an additional factor in determining the rotational motion in multiple inclusion systems, which demands a separate analysis.

We have developed the theoretical model imposing the conditions for mutual mechanical interaction on an elliptical boundary, which is assumed to be a mean line separating the mutually interacting neighbouring inclusions. As a result, the effect of concentration on the rotation behaviour of rigid inclusions shown in this paper is somewhat idealistic in nature. There are some other limitations in the theoretical approach. In its present form the analysis is applicable to inclusion–matrix systems with inclusions axes oriented either parallel or perpendicular to the direction of bulk shear. Moreover, the analysis describes the instantaneous rotation of inclusions and does not remain valid when the inclusions experience significant amounts of rotation after a finite progressive deformation. Evidently, the theoretical results provide just a basis of explaining the effects of inclusion concentration on inclusion rotation observed in physical models. Our principal aim is to show that increasing concentration promotes the rate of antithetic rotation, resulting in the difference in rotation of isolated inclusion and those occurring in a multiple association under a given finite shear. However, in this approach it is not possible to analyse the entire rotation history of multiple inclusions in the experimental models presented here or any natural shear zones. Considering inclusions at an angle to the shear direction, a general theory is required to investigate the course of rotation with progressive shear.

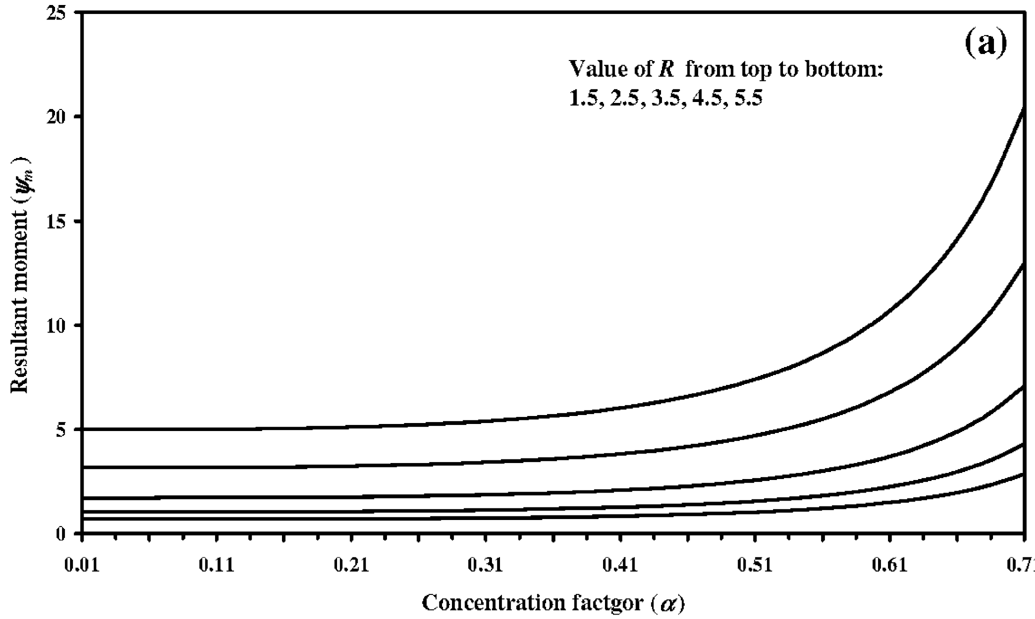

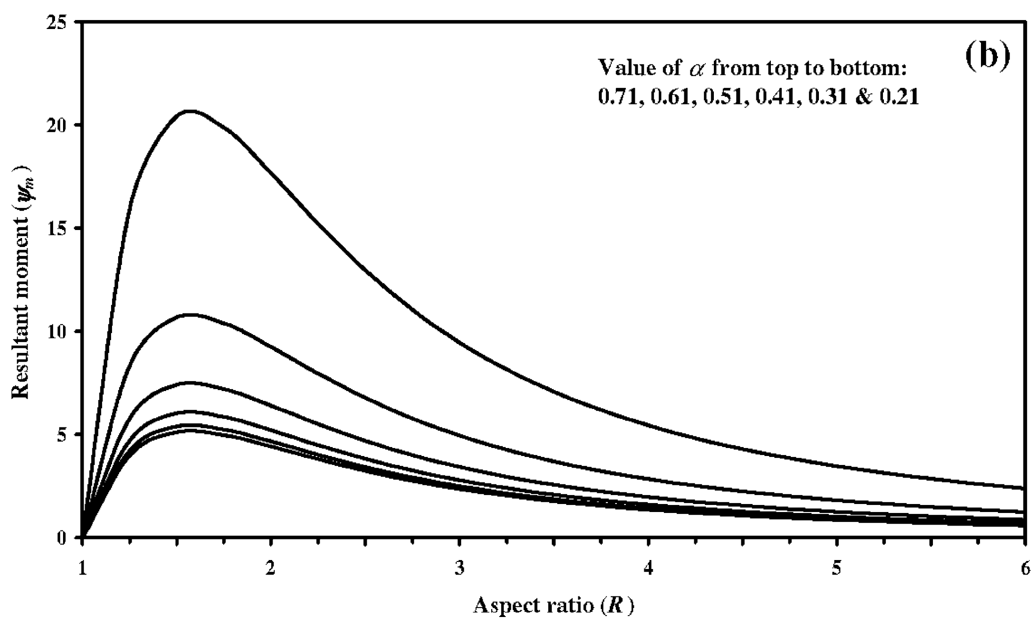

Fig. 14. (a) Non-linear increase of synthetic moment on inclusions with concentration. (b) Variation of synthetic moment with aspect ratio for different values of concentration factor α. Inclusions are initially oriented perpendicular to the shear direction.

Both the experimental and theoretical studies are based on the bulk flow in simple shear. Our analyses are thus applicable to natural shear zones with little or no transpressional or transtensional movements. It has been shown theoretically that shear zones with rigid walls are likely to undergo dominantly shear movement (Mandal et al., 2001b). However, there can be flattening strain in shear zones with deformable walls or involving volume loss (Ramsay, 1980). Rotation of interacting incoherent inclusions in such settings demands further investigation. In this study we have shown that elongate inclusions parallel to the shear direction have a tendency to rotate antithetically and that this tendency is enhanced with increasing inclusion concentration. It can be qualitatively inferred that antithetic rotation would be lower if the shear were accompanied with bulk shortening across the shear direction. In that case inclusions would define a stable fabric at an angle much lower than shown here. In extreme situations inclusions would perhaps remain stationary, as in the case of isolated inclusions with non-lubricated interfaces (cf. Bell, 1985).

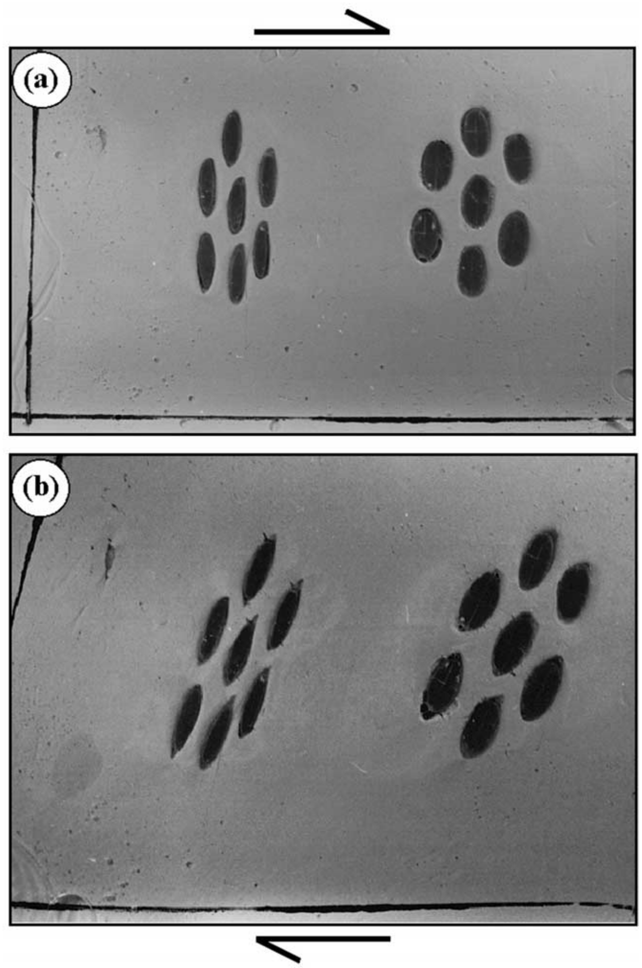

Fig. 15. Test models showing contrasting rotation of multiple inclusions with aspect ratio $R=2$ and $R=4$, oriented perpendicular to the shear direction. Note that the rotation of the inclusions of lower aspect ratio at the centre of the multiple associations (right) is relatively high. Long dimension of inclusions ($R=2$): 2 cm.

In spite of different limitations mentioned above, this study enables us to refine our understanding on a variety of inclusion-associated structures in naturally deformed rocks, such as augen gneisses, mylonites. Mantled porphyroclasts are often used as kinematic indicating structures in natural shear zones (Passchier and Simpson, 1986). The geometry of these structures depends on different physical factors, such as rate of size reduction of porphyroclast, matrix–porphyroclast coherence and rheology of mantle. Our study suggests that increasing inclusion concentration can result in reverse motion of porphyroclasts, especially when the mantle is somewhat rheologically weak, and gives rise to monoclinic mantle structures. On the other hand, porphyroclasts oriented parallel to the shear direction might remain stationary or rotate synthetically where they occur in very low concentrations, and thereby show contrasting mantle geometry. Many deformed rocks show rigid objects showing fissures at the interfaces with the matrix. These fissures are generally filled with either face-controlled or displacement controlled crystal fibres, which are found to be good kinematic indicators (Ramsay and Huber, 1987). According to our model, the geometry of crystal fibres can vary significantly, as both the magnitude and the sense of rotation of inclusion may be different in different domains with varying inclusion concentration. This study will be useful, at least qualitatively to interpret synkinematic fibres in deformed rocks containing inequant clasts in large concentrations. Finally, we believe that our experimental findings can be utilized to explain the orientation of inclusion fabrics that are often noticed in natural shear zones (Ceriani et al., 2003).

5. Conclusions

Based on the experimental findings and theoretical analysis, the outcomes of this study are concluded along the following points:

(1) In multiple inclusion systems, in addition to inclusion–matrix coherence, the concentration of inclusions is a crucial factor in controlling the rotational kinematics of rigid inclusions. Increasing concentration promotes instantaneous antithetic and synthetic rotation of inclusions oriented parallel and perpendicular to the shear direction, respectively.
(2) Isolated inclusions oriented parallel to the shear direction experience little or no rotation when their interfaces are not lubricated, whereas those occurring in multiple association rotate antithetically.
(3) The effective moments in incoherent inclusions oriented parallel to the shear direction are negative, resulting in antithetic motion of inclusions. The magnitude of this antithetic moment is a non-linear function of inclusion concentration, showing a steep increase at large concentrations. Again, when the concentration is kept constant, the moment increases with inclusion aspect ratio, but tends to assume an asymptotic value, suggesting that antithetic rotation will be insensitive to aspect ratio when the latter becomes large.
(4) Increasing inclusion–matrix coherence leads to an overall reduction in the effective antithetic moment of an inclusion oriented parallel to the shear direction. However, the difference in moment resulting from increasing coherence is reduced at high concentrations of inclusions.
(5) In the case of inclusions oriented perpendicular to the shear direction, the effective moment on inclusions is positive, setting in a synthetic motion. Its magnitude increases nonlinearly with inclusion concentration. For a given concentration, the magnitude of synthetic moment increases with aspect ratio to attain a maximum value, and then decreases continuously with further increase in aspect ratio. In multiple inclusion systems, inclusions of large aspect ratios (e.g. 4) are thus likely to

rotate synthetically slower than that of relatively low aspect ratios (e.g. 2).

Acknowledgements

We wish to thank Professors M. Bjornerud, T. Bell and C.W. Passchier for their comments that greatly contributed to the improvement of the paper. We are grateful to the Department of Science and Technology, India for extending financial support in carrying out this work. GB worked with a fellowship of CSIR, India. CC acknowledges the infrastructure supported by the Indian Statistical Institute, Calcutta.

References

Bell, T.H., 1985. Deformation partitioning and porphyroblast rotation in metamorphic rocks: a radical interpretation. Journal of Metamorphic Geology 3, 109–118.

Bell, T.H., Hickey, K.A., 1997. Distribution of pre-folding linear indicators of movement direction around the Spring Hill Synform, Vermont: significance for mechanism of folding in this portion of the Appalachians. Tectonophysics 274, 275–294.

Bell, T.H., Johnson, J.E., 1989. Porphyroblast inclusion trails: the key to orogenesis. Journal of Metamorphic Geology 7, 279–310.

Bjornerud, M.G., Zhang, H., 1995. Flow mixing inclusion matrix coherent mantle growth and the development of porphyroclast tails. Journal of Structural Geology 17, 1347–1350.

Ceriani, S., Mancktelow, N.S., Pennacchioni, G., 2003. Analogue modelling of the influence of shape and particle/matrix interface lubrication on the rotational behaviour of rigid particles in simple shear. Journal of Structural Geology 25, 2005–2021.

Freeman, B., 1985. The motion of rigid ellipsoidal particles in slow flows. Tectonophysics 113, 163–183.

Gay, N.C., 1968a. The motion of rigid particles embedded in a viscous fluid during pure shear deformation of the fluid. Tectonophysics 5, 81–88.

Gay, N.C., 1968b. Pure shear and simple shear deformation of inhomogeneous viscous fluids. 1. Theory. Tectonophysics 5, 211–234.

Ghosh, S.K., Ramberg, H., 1976. Reorientation of inclusions by combination of pure shear and simple shear. Tectonophysics 34, 1–70.

Happel, J., 1957. Viscosity of suspension of uniform spheres. Journal of Applied Physics 28, 1288–1292.

Ildefonse, B., Mancktelow, N.S., 1993. Deformation around rigid particle: influence of slip at the particle/matrix interface. Tectonophysics 221, 345–359.

Ildefonse, B., Launeau, P., Bouchez, J.L., Fernandez, A., 1992a. Effect of mechanical interactions on the development of shape preferred orientations: a two dimensional experimental approach. Journal of Structural Geology 14, 73–83.

Ildefonse, B., Sokoutis, D., Mancktelow, N.S., 1992b. Mechanical interactions between rigid particles in a deforming ductile matrix. Analogue experiments in simple shear flow. Journal of Structural Geology 14, 1253–1266.

Jeffery, G.B., 1922. The motion of ellipsoidal particles immersed in a viscous fluid. Proceedings of the Royal Society of London A 120, 161–179.

Jezek, J., Schulmann, K., Segeth, K., 1996. Fabric evolution of rigid inclusions during mixed coaxial and simple shear flows. Tectonophysics 257, 203–221.

Mancktelow, N.S., Arbaret, L., Pennacchinoni, G., 2002. Experimental observations on the effect of interface slip on rotation and stabilisation of rigid particles in simple shear and a comparison with natural mylonites. Journal of Structural Geology 24, 567–585.

Mandal, N., Samanta, S.K., Chakraborty, C., 2001a. Numerical modeling of heterogeneous flow fields around rigid objects with special reference to particle paths, strain shadows and foliation drag. Tectonophysics 330, 177–194.

Mandal, N., Samanta, S.K., Chakraborty, C., 2001b. Flattening in shear zones under constant volume: a theoretical evaluation. Journal of Structural Geology 22, 1771–1780.

Mandal, N., Samanta, S.K., Bhattacharyya, G., Chakraborty, C., 2003. Deformation of ductile inclusions in a multiple inclusion system in pure shear. Journal of Structural Geology 25, 1359–1470.

Mandal, N., Bhattacharyya, G., Chakraborty, C., 2004. Extensional detachment at the inclusion–matrix interface in a multiple inclusion system. Journal of Structural Geology 26, 1773–1781.

Marques, F.O., Bose, S., 2004. Influence of a permanent low-friction boundary on rotation and flow in rigid inclusion/viscous matrix systems from an analogue perspective. Tectonophysics 382, 229–245.

Marques, F.O., Coelho, S., 2001. Rotation of rigid elliptical cylinders in viscous simple shear flow: analogue experiments. Journal of Structural Geology 23, 609–617.

Masuda, T., Michibayashi, K., Ohata, H., 1995. Shape preferred orientation of rigid particles in a viscous matrix: reevaluation to determine parameters of ductile deformation. Journal of Structural Geology 17, 115–129.

Mushkhelishvilli, N.I., 1953. Some Basic Problems of Mathematical Theory of Elasticity. Noordhoff, Groningen. 704pp.

Passchier, C.W., 1987. Stable positions of rigid inclusions in non-coaxial flow: a study in vorticity analysis. Journal of Structural Geology 9, 679–690.

Passchier, C.W., 1994. Mixing in flow perturbations: a model for development of mantle porphyroclasts in mylonites. Journal of Structural Geology 16, 733–736.

Passchier, C.W., Simpson, C., 1986. Porphyroblast systems as kinematic indicators. Journal of Structural Geology 8, 831–844.

Pennacchioni, G.P., Fasolo, L., Cecchi, M.M., Salasnich, L., 2000. Finite-element modelling of simple shear flow in Newtonian and non-Newtonian fluids around circular rigid particle. Journal of Structural Geology 22, 683–692.

Ramsay, J.G., 1980. Shear zone geometry: a review. Journal of Structural Geology 2, 83–99.

Ramsay, J.G., Huber, M.I., 1987. The Techniques of Modern Structural Geology. Volume 2: Folds and Fractures. Academic Press, London, pp. 491–501.

Samanta, S.K., Bhattacharyya, G., 2003. Modes of detachment at the inclusion–matrix interface. Journal of Structural Geology 25, 1107–1120.

Samanta, S.K., Mandal, N., Chakraborty, C., 2003. Flow patterns around mechanically interacting rigid inclusions under simple shear: theoretical model and geological implications. Journal of Structural Geology 25, 209–221.

Schmid, D.W., Podladchikov, Y.Y., 2004. Are isolated stable rigid clasts in shear zones equivalent to voids? Tectonophysics 384, 233–242.

Stewart, L.K., 1997. Experimental investigation of the effects of fluid heterogeneity upon the motion of rigid ellipsoidal inclusions during bulk inhomogeneous shortening. Journal of Structural Geology 19, 1231–1243.

Treagus, S.H., Lan, L., 2003. Simple shear of deformable square objects. Journal of Structural Geology 25, 1993–2003.